In-plane Strain Measurement by Digital Image Correlation

Po-Chih Hung and A. S. Voloshin
PhotoMechanics Laboratory
Department of Mechanical Engineering & Mechanics
Lehigh University
Bethlehem, PA 18015

This paper presents a "fast and simple" (FAS) detection algorithm based on the digital image correlation for measurement of the surface deformation of planar objects. The proposed algorithm uses only fine search at the pixel level resolution and surface fitting for sub-pixel level. Two different specimens are investigated to explore the feasibility of this proposed algorithm. The displacements calculated by the FAS algorithm are compared with the ones obtained from Newton-Raphson method (N-R) and Enhanced Sequential Similarity Detection Algorithm (ESSDA). The results show that the experimental data are in good agreement with the theoretical solution. The proposed algorithm is found to be much faster than Newton-Raphson method with inferior, yet reasonable, accuracy for displacement and strain evaluation in the cases of uniaxial tension and disk under diametrical compression tests.
***Keywords**: Strain, digital image correlation, speckle*

Introduction

The measurement of displacements and displacement gradients (strains) has always been an important topic in the evaluation of material properties, such as material strengths or fracture parameters and in experimental stress analysis. Optical techniques such as moiré interferometry (Post, 1983), holography (Fottenburg,,1969) and speckle inteferometry (Wang, Chen and Chiang, 1993) have been proven to be matured techniques to analyze macroscopic parameters and are being applied successfully in many different applications. However, all the interferometric techniques have stringent requirements for system's stability. Moreover, the processing of fringe patterns is laborious and time-consuming. This technical difficulty has raised many researchers' attention and computerized procedures (Bastawros and Voloshin, 1990) have been developed to automate the processing of the data from the fringe patterns.

In the last decade, a non-contacting optical technique, digital image correlation, has been developed by Sutton et al. (1983, 1986, 1988, 1991) and Bruck, et al. (1989). It was applied to measurement of displacements and strains. The applications include microscopic strain measurements in electronic packaging (Lu, 1998), strain fields in polyurethane foam plastic materials and evaluation of their mechanical properties (Zhang, Zhang and Cheng, 1999), and evaluation of thermal strain in the solder joints (Lu, Yeh and Wyatt, 1998). This methodology was even used for in situ evaluation of the state of conservation of mural frescoes (Spagnolo, et al., 1997). This computer vision technique has the advantages of a simple system and direct sensing and thus avoids the laborious interpretation of interferometric fringes. The technique utilizes two similarly speckled images, which were captured by a solid state video camera, to represent the states of the object before and after deformation. By utilizing the concept of digitalization, one can characterize the image by the patterns of different levels of light intensity. Both of the digitized images are then correlated by an algorithm, based on their mutual correlation coefficient or other statistical functions, to find out the subtle differences between them.

The core of digital image correlation in this application depends on the ability to recognize two nearly similar, yet different, image patterns. Nevertheless, one could always use brute force (blanket method) to correlate both images grid by grid to their desired accuracy (Cardenas-Garcia, Yao and Zheng, 1993), but the consumption of CPU time would be enormous and impractical. Therefore, an efficient method to optimize the algorithm is needed to carry out the image correlation. A decade ago, an improved algorithm, Newton-Raphson method with partial differential correction, was used and it was shown that the computation of correlation has been drastically decreased in comparison with the coarse-fine search algorithm (Bruck, et al., 1989). Their methodology assumes that the local deformation is uniform and therefore the local deformation could be represented by two displacements and four displacement gradients, or so called direct strains. The Newton-Raphson method can provide fast convergence in searching for the local minimum with high accuracy, but the displacement gradients (direct strains), found in the best-matching pattern, are still shown to have a large variability (Bruck, et al., 1989). Therefore it was suggested that the strains derived from displacement functions should be more accurate than direct strains. Their work showed that an accuracy of ±0.05 pixel in two-dimensional displacement measurements could be achieved if one uses an 8-bit digitizer. A further improvement could be achieved if a 12-bit digitization is used (Sutton et al., 1988).

In spite of the great improvement in the convergence speed, the Newton-Raphson method with partial differential correction still suffers from significant consumption of computation time in detecting the local minimum. A simple search algorithm, which will allow approach of digital image correlation more applicable for practical use, is proposed here. The proposed algorithm uses fine search (pixel by pixel) on the pixel level with fixed area. The location of the local minimum on sub-pixel level is then decided based on the fitting surface to the range of discrete pixels surrounding the solution on the pixel level. The accuracy of experimental results from this proposed algorithm may not to be superior to the Newton-Raphson method with partial differential correction. However, the experimental results show that the detection speed is increased sufficiently while the degradation in accuracy was acceptable for practical use.

Nomenclature

A(i,j), B(i,j) = light intensity at location i,j
B, a, r = matrixes in equation (4)
i,j = location in the reference image
i^*,j^* = location in the deformed image
f(x,y) = fitting surface
m,n = subset size in pixels
p = nearest location
r(i,j) = mutual cross coefficient
u, v = the displacement of the pixel

Paper accepted June, 2003. Technical Editor: Atila P. Silva Freire.

Digital Image Correlation

Digital image correlation is an application based on the comparison of two images acquired at different states, one before deformation and the other one after. These two images are referred as reference and deformed images in the scope of this paper. After acquisition by a CCD camera, these images are digitized and stored in a computer hard disk for analyses. Two subsets are chosen respectively from the reference and deformed images for correlation. The algorithm of correlation, detecting the local displacements **u** and **v** by comparing the two image subsets, is as follows.

The interested point in the reference image is characterized by a rectangular subset, an (n x m) pixel area. The corresponding subset, also an (n x m) pixel area, in the deformed image is estimated at a certain location with a specified range. A fine search routine, pixel by pixel, is performed within the specified range in the deformed image. The nearest location p at the pixel level, as shown in Fig.1, is selected based on the occurrence of the best-matched pattern (Press, et al., 1992), which has the minimum value of mutual cross coefficient r(i,j).

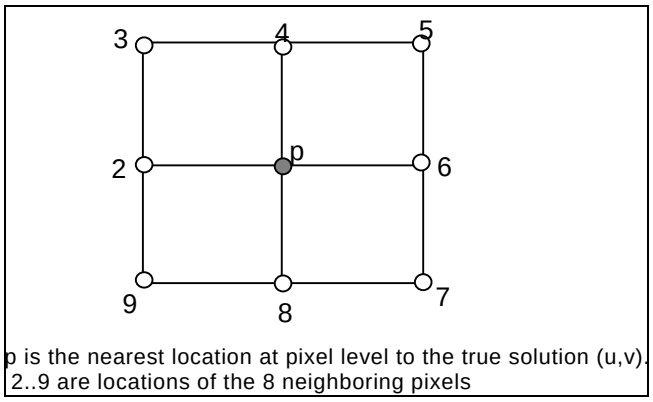

Figure 1. Pixel level solution (p) and its neighbors.

$$r(i,j) = 1 - \frac{SA(i,\ j)B(i^*, j^*)}{(SA(i,\ j)^2 * SB(i^*, j^*)^2)^{1/2}} \qquad (1)$$

where A(i , j) is the gray level at the location of (i , j) in the reference image A,

B(i* , j*) represents the gray level at the location of (i* , j*) in the deformed image B.

The relationship between (i , j) and (i* , j*) could be described as follows.

$$i^* = i + u\ ,\ j^* = j + v \qquad (2)$$

where u, v represent the displacement of the pixel of (i , j) in the horizontal and vertical directions, respectively.

The next step is to decide the exact values of u and v. The selected most nearest location **p** and its eight neighboring pixel locations will constitute a fitting surface that can be represented by a two dimensional quadratic function f(x,y).

$$f(x,y) = a_1x^2 + a_2y^2 + a_3xy + a_4x + a_5y + a_6 \qquad (3)$$

It is assumed that the displacements u and v could be defined based on the location of the minimum value of the fitting surface. Thus, to find the values of u and v requires solving a set of nine linear equations,

$$\mathbf{B} \cdot \mathbf{a} = \mathbf{r} \qquad (4)$$

where **B** is a 9x6 matrix, consisting of the evaluation of each term in function f(x,y),

a is a 6x1 vector, representing the unknown coefficients $a_1..a_6$,

r is a 9x1 vector consisting of the evaluation of r(i , j) at the locations as described in Figure 1. Since the number of unknowns is less than the number of the equations, one is expected to find the least-squares solution to this overdetermined set of linear equations. This equation set is solved by using a numeric technique SVD (Press, et al., 1992), singular value decomposition, to decompose the matrix **B**. The evaluations of **u** and **v** can be obtained by solving the following linear equations,

$$\begin{cases} \partial f\ /\ \partial x = 0 \\ \partial f\ /\ \partial y = 0 \end{cases} \qquad (5)$$

The displacement fields of **u** and **v** can then be determined simply by substituting different **r** vector into the above iterating process.

Experimental Validation

In order to create a characteristic pattern on the specimen surface, the specimen was sprayed by a white paint to obtain a white background. Black speckles were then deposited on the white surface by randomly spraying the black paint on the background. The testing specimen then was installed into a loading frame and speckle patterns were acquired at various loading conditions. In order to verify the validity range of the proposed numerical algorithm for digital image correlation, three basic tests: inherent error estimation, translation and rotation, were performed.

Inherent errors

The first experiment, static error estimation, was designed to evaluate the inherent errors incurred by signal and lighting variation. The reference and deformed images are acquired at a static state without external loading or movement. An averaging technique is applied to the correlation process. This averaging procedure was to divide the sum of n (≤ 50) multiple images by n. The time of averaging an image 50 times is about five seconds. The detected errors are calculated by $(\delta x^2 + \delta y^2)^{1/2}$, where δx and δy are the detection error in the horizontal and vertical directions, respectively. Experimental results show that the inherent errors are not decreased by increasing the number of averaging times, as shown in Fig. 2. The comparison between no averaging and averaged 50 times is presented in the Table 1.

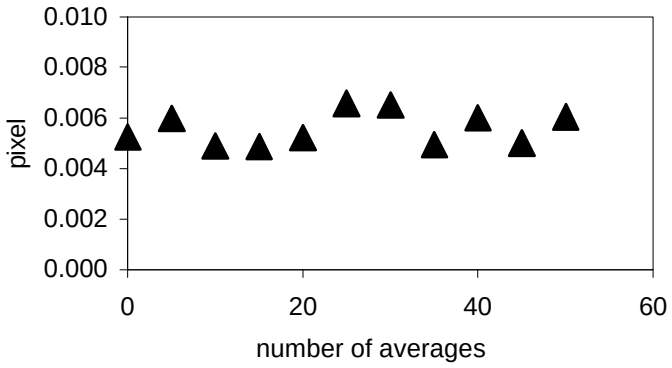

Figure 2. Inherent error versus number of averages in FAS algorithm.

Table 1. Inherent errors due to the signal and lighting variation.

Deformation Parameters	u (pixel)	v (pixel)	∂u/∂x	∂u/∂y	∂v/∂y	∂v/∂x
Both images with no averaging	0.00518 ±0.0017	-0.00496 ±0.00124	0.000543 ±0.000433	-0.000277 ±0.000306	0.000596 ±0.000261	-0.000160 ±0.000208
Both images averaged 50 times	0.002257 ±0.001449	-0.006464 ±0.000519	0.000482 ±0.000720	0.000396 ±0.000252	0.000297 ±0.000399	-0.000095 ±0.000167

Translation Test

The second experiment, translation test, was designed to evaluate the accuracy of a rigid body translation. The specimen with speckled pattern was translated at an increment of 0.005 mm. The resolution of this optical setup was 0.069 mm/pixel, which means that each increment was about 0.072 pixel. Experimental results, as shown in Fig. 3, show that the predicted displacements are in good agreement with the actual translation.

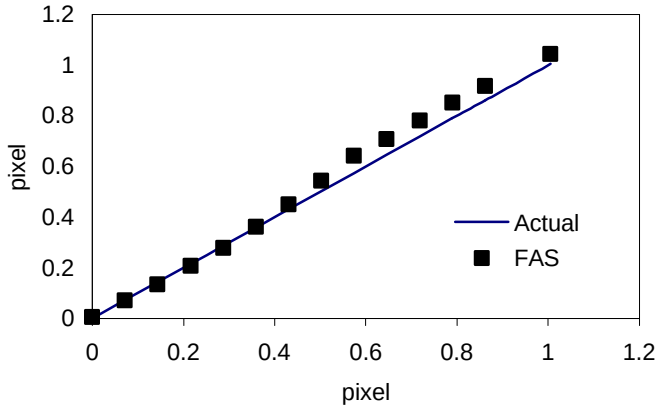

Figure 3. Experimental results for the translation tests (an increment of 0.072 pixel).

In-Plane Rotation Test

Since the algorithm proposed here matches the images with the fixed rectangular areas, the influence of in-plane rotation is predicted to be significant. The specimen with speckled pattern was rotated about the z-axis at an increment of 1° until 10° angle was reached. Experimental results show that the prediction of rotation angle is valid until the actual rotation is more than 7°, as shown in Fig. 4. At this orientation, the specified area starts to lose its perceptiveness and the search wanders off, which results in detection of the wrong displacements. This is clearly seen from the plots of the correlation profiles for the case of one (Fig. 5a) and eight (Fig. 5b) degrees of the sample rotation. It could be easily observed that at the eight degrees of rotation there is no obvious peak in the correlation profile when comparing to the correlation profile corresponding to one degree of rotation.

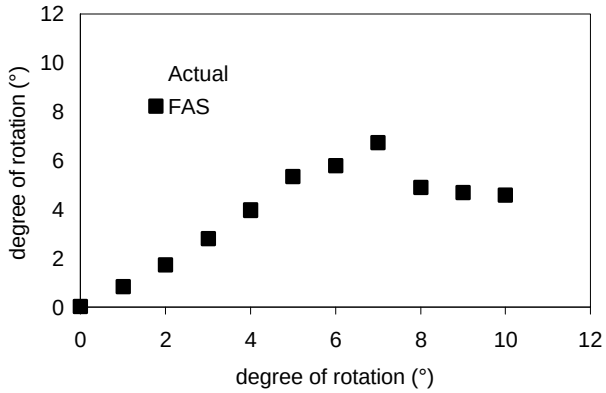

Figure 4. Experimental results for the rotation tests.

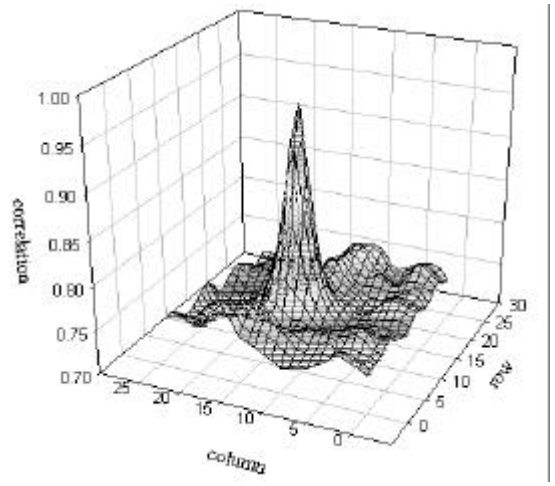

(a)

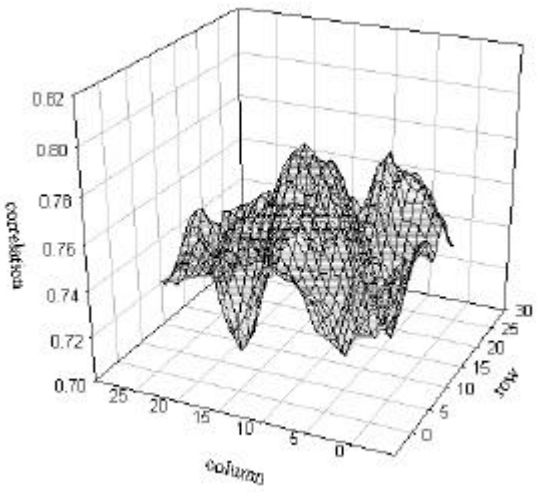

(b)

Figure 5. Effect of the image rotation on the correlation function. a) rotation of one degree; b) rotation of eight degrees.

Tension Test

An aluminum plate was machined to a dog-bone like specimen for a uniform uniaxial tension test. The length of the specimen was 115 mm with a cross sectional area of 28 mm^2. Three strain gages were mounted on one side of the specimen and placed at angles of 0^0, 45^0 and 90^0 with respect to the loading axis. Each one of the three strain gages was arranged in a quarter Wheatstone bridge, respectively, so that an early detection of misalignment between the specimen direction and the loading axis could be detected by monitoring the shear strain γ at the gage location.

$$g = 2e_{45} - e_0 - e_{90} \tag{6}$$

In the case of the pure axial loading the shear strain should be zero.

On the other side of the specimen was painted randomly to yield a speckled pattern. The specimen was installed into an INSTRON, model 1011. During the loading history the speckled pattern and the readings of strain gages were recorded. Two conspicuous makers, along the loading axis, on the speckled surface were also recorded in the images during the test. The initial distance between these two makers was about 400 pixels long so it was possible to estimate the average strain in the specimen by measuring the relative difference in their positions. Newton-Raphson method and FAS algorithm were applied to correlate five discrete image subsets from the reference and deformed image. The linear regression approach was used to smooth the measured data. The experimental results are illustrated in Fig. 6.

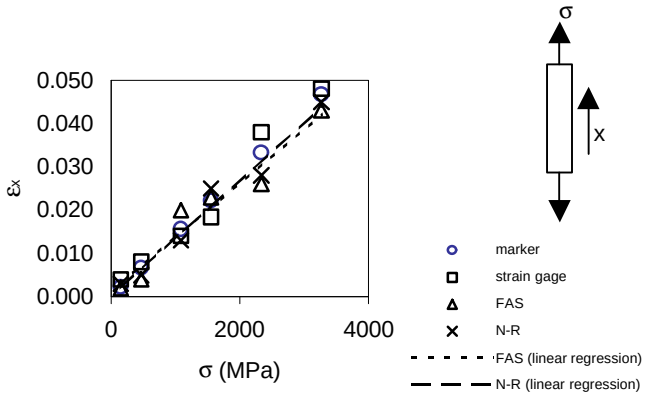

Figure 6. Aluminum specimen under axial load. Longitudinal strains by FAS algorithm, Newton-Raphson method, relative makers' position and strain gages are shown vs. applied stresses.

Compression test

A circular disk made from Plexiglas was installed into an INSTRON and diametrical compression was applied to it as shown in Fig. 7. The speckle images at different loading stages were recorded. The random speckle pattern as it was recorded before the application of the load is shown in Fig. 8. Three different algorithms were used to calculate the strains: Newton-Raphson method, ESSDA (Umezaki, Shimamoto and Watanabe, 1993) and FAS method for comparison. Since the computational results from ESSDA showed large inconsistency, therefore only the results of Newton-Raphson and FAS are compared with theoretical solutions (Mal and Singh, 1991). The experimental results for ε_x, ε_y, γ_{xy} and the corresponding theoretical solution are illustrated in Figs. 9, 10 and 11. Relatively large deviation of the calculated strain ε_x (Fig. 9) from the theoretical predictions at about 10 mm from the disk center may be attributed to the speckle quality and size distribution at this particular location. The computation time for each algorithm is listed in Table 2. It should be noted that those times show only relative performance of one algorithm versus another and not an absolute time, which may be dependent on the number of factors, like programming efficiency, use of language, etc.

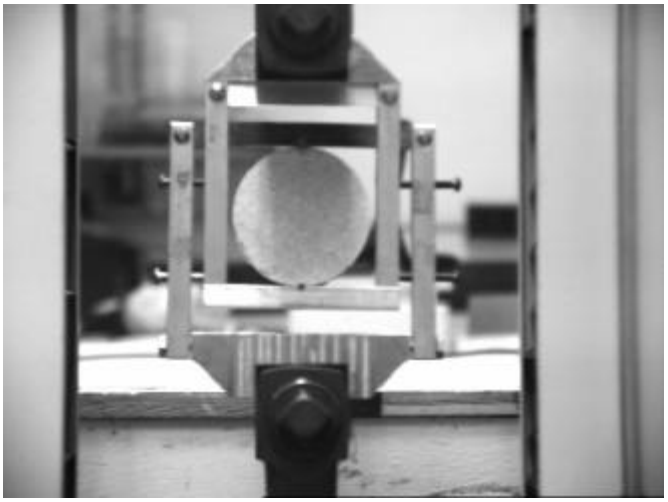

Figure 7. Plexiglas disk under diametrical compression.

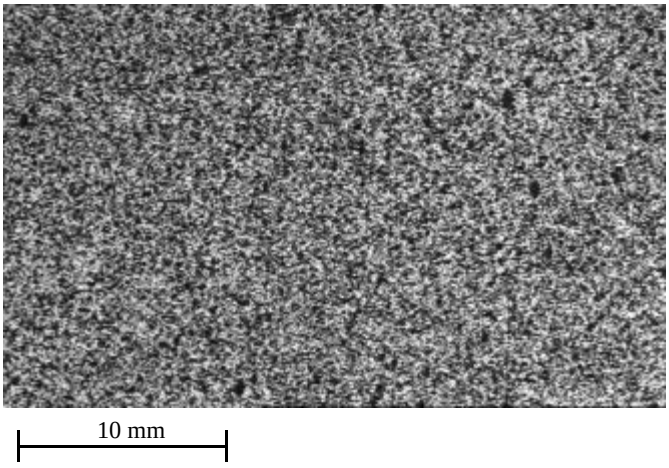

Figure 8. Random speckle pattern applied to the disk.

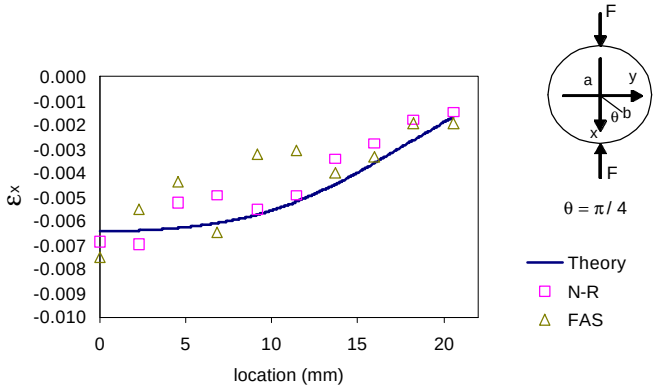

Figure 9. Strain ¶u/¶x along the line ab at a circular disk subjected to 3910 N.

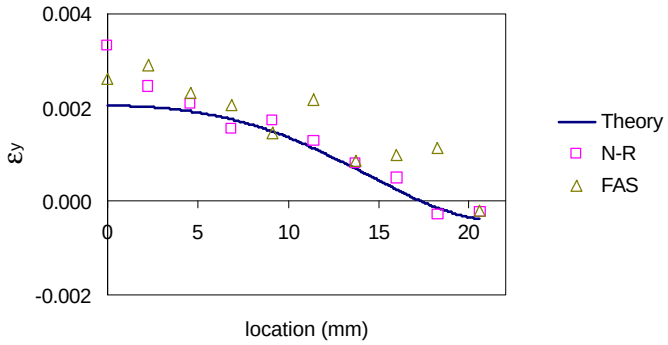

Figure 10. Strain ¶v/¶y along the line ab at a circular disk subjected to 3910 N.

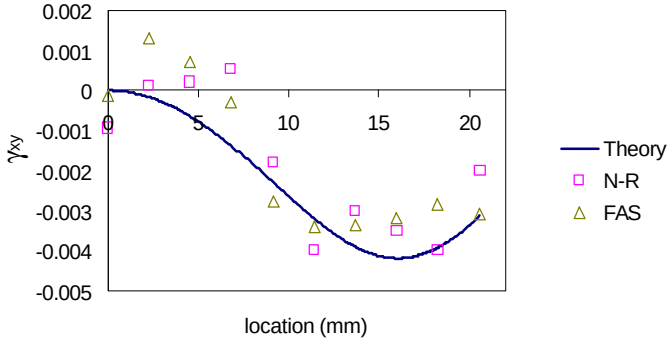

Figure 11 Strain (¶u/¶y + ¶v/¶x) along the line ab at a circular disk subjected to 3910 N.

Table 2. The CPU consumption for each algorithm is measured on a PC System with an Intel Pentium II 300 MHz processor. The consumed time for N-R algorithm is computed based on an average of 9 iterations for each point.

A 14 x 14 area	Newton-Raphson	ESSDA	FAS
CPU (second)	600	1.54	1.5

Speckle Size

The average size of speckles and its distribution in the random pattern plays an important role in these similarity-searching algorithms. It was found, through testing that the speckles should be two to three pixels in size, when imaged by the video camera, in order to achieve satisfactory correlation results by using the coarse-fine search method (Bruck et al., 1989). Nevertheless, the influence of the average speckle size is expected to be more significant in the FAS algorithm because it lacks the ability to adjust the dimensionality or shape of the target window with respect to the corresponding deformation. Therefore an investigation of strains against different speckle sizes was performed. Figure 12 shows the calculated result of a normal strain εx with respect to different average speckle sizes in the uniaxial tension test. The variety in average speckle size was obtained by equally resizing both dimensions of the original pattern of the acquired image, either by dezooming or zooming. The bicubic interpolation process was adapted for zooming the pattern, while the averaging method was used for dezooming. The average speckle size was sampled from each image and calculated using digital image processing procedures (Matrox Image Processing, 1997). The speckle size analysis was performed by binarizing the images, based on their thresholds, and then measuring and averaging speckle diameters at various cross-sections.

The study of the effects of the speckle size on the measured strain was performed for two normal strain values: 0.046 and 0.0029. The sample from the above describes tensile test was used for this analysis. The sample was loaded until the desired normal strain was achieved, as measured by the strain gages. The strain was calculated at five randomly selected locations near the center of the sample. The average of these five values is shown in Fig. 12 (solid line) for the range of speckle sizes (2-14 pixels). It is found that, at a mean strain of 0.046, the calculated strain starts to deviate from the applied strain when the average speckle size is greater than ten pixels. A similar investigation was performed for a mean strain of 0.0029 and the results are shown in Fig. 13. The deviation of data from mean strain happens when the average speckle size is less than two pixels. These results indicate that the appropriate speckle size in the uniaxial tensile test should fall between two and ten pixels for accurate measurement of the normal strain in the range of 0.0029 to 0.046.

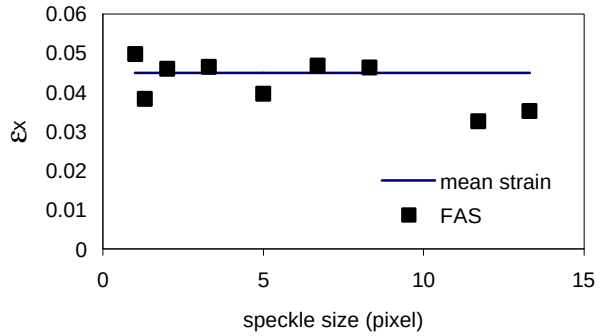

Figure 12. Strain ε_x measured by FAS with respect to different speckle sizes in uniaxial tension test.

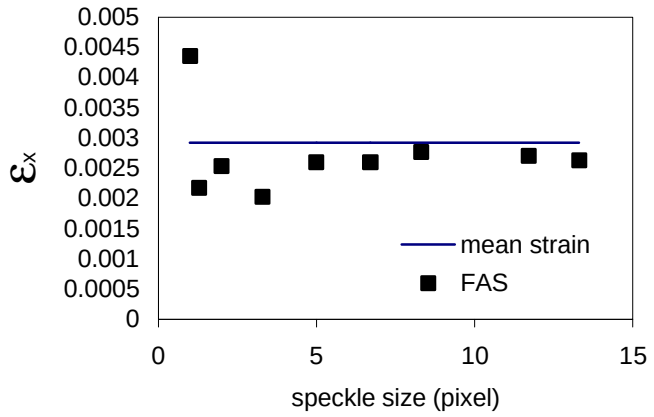

Figure 13. Strain e_x measured by FAS with respect to different speckle sizes in uniaxial tension test.

However, presence of the shear strain will lead to the distortion of the target window and, therefore, could put stricter requirements on the validity of the average speckle size. The effect of the average speckle size on the calculated strains, in a disk subjected to diametrical compression test, is shown in Figs. 14, 15 and 16. It is found from this analysis that to achieve a reasonable correlation results the average speckle diameter should be four to seven pixels.

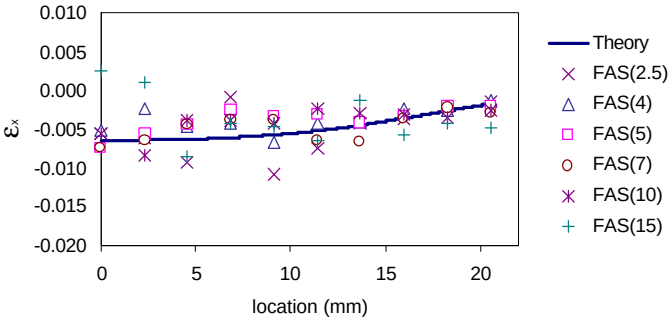

Figure 14. Strain e_x measured by FAS with respect to different speckle sizes (in pixels) in diametrical compression test.

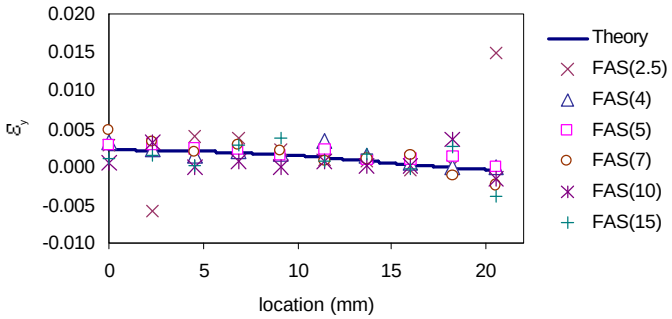

Figure 15. Strain e_y measured by FAS with respect to different speckle sizes (in pixels) in diametrical compression test.

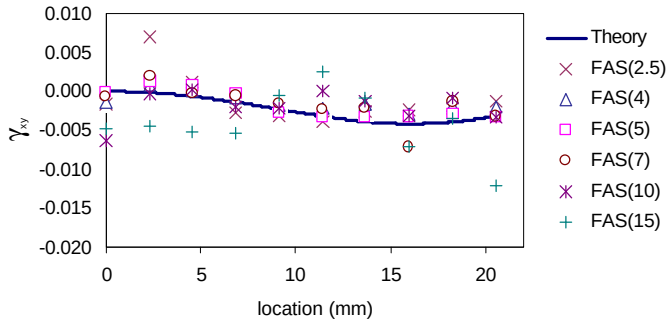

Figure 16. Strain g_{xy} measured by FAS with respect to different speckle sizes (in pixels) in diametrical compression test.

When speckle size is reduced to less than two pixels, its actual location and light intensity will have higher uncertainty than that for a speckle of larger size. The main reason is that the effect of a given speckle (its perceived location and brightness) will be different depending on its position. Let us consider two extreme cases. When speckle center falls on the center of a pixel, it will be sensed by nine pixels, as schematically shown in the Fig. 17a, while when its center falls on the corner of a pixels – it will be sensed by only four pixels (Fig. 17b). Thus, for a small speckle of only two pixels in diameter, it will lead to greater errors in the determination of the speckle location and average light intensity. For the speckle of a larger size these errors will be minimized. However, when speckle size becomes too large, the ability to accurately measure smaller strains will be diminished.

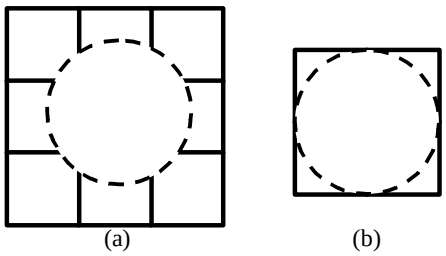

Figure 17.Schematic of the possible locations for the small speckle (dashed line) with respect to the pixel (solid line). (a) speckle center coincides with the pixel center. (b) speckle center coincides with the corner of the pixel.

Discussion

The area-based algorithm for digital image correlation, described in this work, is a technique utilizing the image pixel correspondence with fixed areas. Since the specified area is fixed through out the correlation process, two important factors that will affect the correlation accuracy need to be noted. Firstly, the quantity of geometric distortion within the target area in the deformed image must be small enough not to inhibit the matching of the speckled patterns. Secondly, the magnitude of gray level variations within the specified area must be sufficiently large to provide the required characteristics for local similarity of the image parts. The variation of gray levels could be increased by increasing the size of the specified area. However, the effects of perspective geometric distortion could be minimized through smaller specified areas. Therefore, the decision about the dimensionality of the specified area has to accommodate the consideration of these two conflicting factors. Currently there is no systematic method to access this problem. Hence the optimized dimensionality in this research was decided on a trial and error basis.

In order to reduce the computational errors, most applications of digital image processing do perform an averaging of the images to filter out the optical noise and electrical signal variation. However, from the experimental results of the inherent errors, based on different averaging number, it appears that the inherent errors are insensitive to the averaging method and the errors are kept at an approximate value of 0.005 pixel.

The experimental data of baseline test for rigid body translation shows that the calculation of displacements could be as accurate as 0.07 pixel in this optical setup. The rotation test was used to evaluate the influence of $\partial u/\partial y$ and $\partial v/\partial x$ on correlation. The experimental results show that the calculations for rotation are valid only until 7°. However, with the combination of other deformations, $\partial u/\partial x$ and $\partial v/\partial y$, the applicability of this algorithm could be affected significantly.

In the uniaxial test for ε_x ranging from 0.0029 to 0.046 the average error, after smoothing, was found to be about 5.8%. However, in the diametrical compression test the average errors for strain measurement were found to be higher. The local distortions and deviations in the speckle size were considered to be the major contributions to the measurement errors. Significant deviation of the calculated strain ε_x (Fig. 9) from the theoretical predictions at about 10 mm from the disk center may be attributed to the speckle quality and size distribution at this location. Nevertheless, the majority of measured strain values (ε_x, ε_y and γ_{xy}) show a reasonably good agreement with the theoretical predictions (Figs. 9, 10 and 11).

Conclusions

This research presents an analysis of an area-based image matching technique under geometric distortion. The translation and rotation baseline tests show the precision and limitations of this algorithm. However, it should be noted that with the existence of large distortions, the specified area is liable to lose its perceptiveness in recognizing the target area. In such case, the detection of displacements may wander off and hence the precision of this method would be reduced significantly.

The inherent errors of using the proposed algorithm to correlate two speckled patterns were also analyzed. The experimental data from the tensile test show good agreement with the readings of strain gages in the range from 0.0029 to 0.046. This result indicates that for the uniform tension test, this method is a very convenient, fast, and efficient tool. Less accuracy was achieved in a disk under diametrical compression test. Therefore the proposed here approach may not be applicable when accurate data is required and the processing time is not a problem. However, the facts that the errors are not sensitive to the averaging technique and the relatively small consumption of the computational time in detecting the displacements and strains suggest that this method has a potential for online quality analysis where time is of essence.

References

Bastawros, A. F. and Voloshin, A. S. Thermal Strain Measurements in Electronic Packages through Fractional Fringe Moiré Interferometry. *Journal of Electronic Packaging*, 1990, 112(4), 303-308.

Bruck, H. A., McNeil, S. R., Sutton, M. A. and Peters, W. H. Digital Image Correlation Using Newton-Raphson Method of Partial Differential Correction. *Experimental Mechanics*, 1989, 29(3), 261-267.

Cardenas-Garcia, J. F., Yao, H. and Zheng, S. Elastic Strain Measurement Using Digital Image Correlation. In Proceedings of Conference On Advanced Technology in Experimental Mechanics, JSME, 1993, pp. 167-172.

Fottenburg, W. G. Some Applications of Holographic Interferometry. *Experimental Mechanics*, 1969, 8, 281-285.

Lu, H. Applications of digital speckle correlation to microscopic strain measurement and materials' property characterization. *Journal of Electronic Packaging, 1998*, 120 (3), 275-279.

Lu, H., Yeh, C. and Wyatt, K. Experimental evaluation of solder joint thermal strain in a CSP using digital speckle correlation, 1998, Thermomechanical Phenomena in Electronic Systems -Proceedings of the Intersociety Conference, IEEE, Piscataway, NJ, USA, 98CH36208, 241-245.

Mal, A. K. and Singh, S. J. Deformation of Elastic Solids. 1991, pp. 231-232 (Prentice Hall, NJ).

Matrox Image Processing Group. Matrox Imaging Library, 1997, v5.0, pp. 14.

Post, D. Moiré Interferometry at VPI and SU. *Experimental Mechanics*, 1983, 23(2), 203-210.

Press, W. H., Teukolsky, S. A., Vetterling W. T. and Flannery, B. P. Numerical Recipes in C. Published by Cambridge University Press, 1992, pp. 636.

Spagnolo, G., Schirripa, Paoletti, D., Ambrosini, D. and Guattari, G. Electro-optic correlation for in situ diagnostics in mural frescoes. *Pure & Applied Optics: Journal of the European Optical Society*, 1997, Part A. 6 (5), 557-563.

Sutton, M. A., Wolters, W. J., Peters, W. H., Ranson, W. F. and McNeil, S. R. Determination of Displacements Using an Improved Digital Correlation Method. *Image and Vision Computating*, 1983, 1(3), 133-139.

Sutton, M. A., Cheng, M. Q., Peters, W. H., Chao Y. J. and McNeill, S. R. Application of an Optimized Digital Correlation Method to Planar Deformation Analysis. *Image and Vision Computing*, 1986, 4(3), 143-151.

Sutton, M. A., Turner, J. L., Bruck, H. A. and Chae, T. A. Full-field Representation of Discretely Sampled Surface Deformation for Displacement and Strain Analysis. *Experimental Mechanics*, 1991, 31(2), 168-177.

Sutton, M. A., McNeill, S. R., Jang, J. and Babai, M. Effects of Sub-pixel Image Restoration on Digital Correlation Error. *Journal of Optical Engineering*, 1988, 27(10), 870-877.

Umezaki, E., Shimamoto, A. and Watanabe, H. Improvement in Speed and Accuracy of Digital Image Correlation Method. In Proceedings of Conference on Advanced Technology in Experimental Mechanics, JSME, 1993, pp. 173-178.

Wang, Y. Y., Chen, D. J. and Chiang, F. P. Material testing by computer aided speckle interferometry. *Experimental Techniques*, 1993, 17(5), 30-32.

Zhang, D. Zhang, X. Cheng, G. Compression strain measurement by digital speckle correlation. *Experimental Mechanics, 1999*, 39 (1), 62-65.